Published in final edited form as:
J Pharmacol Toxicol Methods. 2012 March ; 65(2): 64–74. doi:10.1016/j.vascn.2012.02.002.

Determining P-glycoprotein-drug interactions: evaluation of reconstituted P-glycoprotein in a liposomal system and LLC-MDR1 polarized cell monolayers

Donald L. Melchior[*,a], **Frances J. Sharom**[b], **Raymond Evers**[c], **George E. Wright**[a], **Joseph W.K. Chu**[b], **Stephen E. Wright**[a], **Xiaoyan Chu**[c], and **Jocelyn Yabut**[c]

[a]GLSynthesis Inc., One Innovation Drive, Worcester, Massachusetts 01605 USA

[b]Department of Molecular and Cellular Biology, University of Guelph, Guelph Ontario N1G 2W1, Canada

[c]Drug Metabolism and Pharmacokinetics, Merck and Co Inc., P.O. Box 2000, Rahway, New Jersey 07065 USA

Abstract

Introduction—P-Glycoprotein (ABCB1, MDR1) is a multidrug efflux pump that is a member of the ATP-binding cassette (ABC) superfamily. Many drugs in common clinical use are either substrates or inhibitors of this transporter. Quantitative details of P-glycoprotein inhibition by pharmaceutical agents are essential for assessment of their pharmacokinetic behavior and prevention of negative patient reactions. Cell-based systems have been widely used for determination of drug interactions with P-glycoprotein, but they suffer from several disadvantages, and results are often widely variable between laboratories. We aimed to demonstrate that a novel liposomal system employing contemporary biochemical methodologies could measure the ability of clinically used drugs to inhibit the P-glycoprotein pump. To accomplish this we compared results with those of cell-based approaches.

Methods—Purified transport-competent hamster Abcb1a P-glycoprotein was reconstituted into a unilamellar liposomal system, Fluorosome-*trans*-pgp, whose aqueous interior contains fluorescent drug sensors. This provides a well-defined system for measuring P-glycoprotein transport inhibition by test drugs in real time using rapid fluorescence-based technology.

Results—Inhibition of ATP-driven transport by Fluorosome-*trans*-pgp employed a panel of 46 representative drugs. Resulting IC_{50} values correlated well ($r^2 = 0.80$) with K_d values for drug binding to purified P-glycoprotein. They also showed a similar trend to transport inhibition data obtained using LLC-MDR1 cell monolayers. Fluorosome-*trans*-pgp IC_{50} values were in agreement with published results of digoxin drug-drug interaction studies in humans.

Discussion—This novel approach using a liposomal system and fluorescence-based technology is shown to be suitable to study whether marketed drugs and drug candidates are P-glycoprotein inhibitors. The assay is rapid, allowing a 7-point IC_{50} determination in <6 minutes, and requires minimal quantities of test drug. The method is amenable to robotics and offers a cost advantage

[*]**Corresponding author:** Donald L. Melchior, GLSynthesis Inc., One Innovation Drive, Worcester, Massachusetts 01605 USA, Donald.Melchior@glsynthesis.com, phone: +1 508 754 7075, fax: +1 508 754 7075.

relative to conventional cell-based assays. The well-defined nature of this assay also obviates many of the inherent complications and ambiguities of cell-based systems.

Keywords

ABCB1; drug transport; drug interaction; fluorescence; inhibitor; liposome; methods; polarized cell monolayer; reconstitution

1. Introduction

Several mammalian members of the ATP-binding cassette (ABC) superfamily of proteins function as multidrug efflux pumps (Eckford & Sharom, 2009). These proteins not only serve to protect the organism from potentially toxic xenobiotics, but also play an important role in the absorption and distribution of drugs used in clinical therapy (Leslie, Deeley, & Cole, 2005). Of the ABC multidrug transporters, P-glycoprotein (Pgp; ABCB1, MDR1) is the most studied, and the one we know most about in terms of its structure and mechanism of action. Pgp substrates vary widely in their molecular structure, although most are 300–1000 Da in size, amphipathic and relatively non-polar, often with aromatic rings and a positive charge at physiological pH. Substrates of Pgp are transported out of the cell in an ATP-dependent fashion, and *in vitro* studies have shown that this transport is active and takes place against a chemical gradient of substrate concentration (reviewed in Sharom, 1997). Pgp is localized in the apical plasma membrane of intestinal epithelial cells, where it limits entry of substrates from the gut lumen, and at the apical surface of endothelial cells in the capillaries of the brain (Eckford & Sharom, 2009). Here, it forms a major component of the blood-brain barrier, impeding the entry of substrates into the central nervous system. Studies on Pgp knockout mice have confirmed the physiological role of Pgp in these tissues, and have also been useful in assessing how the transporter handles many pharmacological agents (Schinkel, 1998).

Pgp inhibitors (also known as modulators) also interact with the protein, but they block the transport process. Inhibitors share many of the chemical properties of transport substrates, and are also structurally diverse. Many drugs in common clinical use are either substrates or inhibitors of Pgp, including anticancer drugs, calcium channel blockers, HIV protease inhibitors, calmodulin antagonists, anti-histamines, analgesics, steroids, antibiotics, and immunosuppressive agents (for a more detailed list, see Sharom, 2008; Eckford & Sharom, 2009). Because of the involvement of Pgp in the intestinal absorption and tissue distribution of these drugs, their effectiveness may be adversely affected by interaction with the transporter. In addition, pharmacokinetic interactions between two drugs that both interact with Pgp can be a serious problem potentially leading to toxic side effects in patients. Because a large number of pharmaceutical agents interact with Pgp, it is important to test new drugs for such interactions and also to establish whether existing drugs in clinical use are substrates or inhibitors of the transporter. The U.S. Food and Drug Administration now recommends that Pgp-interactions be documented as part of the drug approval process (Giacomini et al., 2010). Attempts have been made to develop pharmacophores for Pgp, however, experience has shown that, at best, these work within a structural series, and that extrapolations to structurally unrelated compounds are not possible. Therefore, reliance on *in silico* approaches to determine whether compounds are substrates or inhibitors of Pgp is not currently feasible. This emphasizes the need for the development of higher throughput experimental assays, as exemplified in the present manuscript.

A large number of *in vitro* and cultured cell-based assays have been developed for assessing the interaction of drugs with Pgp (for a review, see Sharom & Siarheyeva, 2008). Many of these methods are based on inhibition of transport of a reference compound by the test drug,

to produce an IC_{50} value. Each of the methods in current use has shortcomings, and a combination of approaches is often needed to unambiguously identify Pgp substrates and inhibitors. Methods based on polarized epithelial cell monolayers are widely used, and considered the "gold standard" in the pharmaceutical industry. Yet these assays are expensive, time-consuming, and labor-intensive (Polli et al., 2001). All cell lines express other drug transporters in addition to Pgp (Acharya et al., 2008), and sometimes carry out metabolism of the test drug, making interpretation of results more difficult. Also, as described in the Discussion section of this paper, the IC_{50} values obtained from cell-based assays are often highly variable between laboratories.

In this work, we sought to demonstrate that a novel experimental approach utilizing contemporary biochemical methodology incorporating highly purified, functionally reconstituted Pgp into liposomal particles with fluorescent sensor molecules in their interiors can quantitate inhibition of Pgp-mediated transport by test drugs in real time. We also evaluated whether measured IC_{50} values for a panel of 46 drugs using this *in vitro* system correlate with the affinity of these compounds for binding to purified Pgp, and whether the results for a subset of these compounds are similar to those obtained from cell monolayer experiments. The IC_{50} values are also correlated with *in vivo* published data on drug interactions with digoxin.

2. Materials and methods

2.1 Materials

Hamster Abcb1a Pgp was purified from plasma membrane vesicles of the multidrug-resistant cell line $CH^{R}B30$, as previously described (Liu, Siemiarczuk, & Sharom, 2000). The final product was 90–95% pure protein in 2 mM 3-[(3-cholamidopropyl)dimethylammonio]-1-propanesulfonate (CHAPS), with ATPase activity in the range 1.5–2.1 μmol/min per mg protein, as determined by an assay described earlier (Eckford & Sharom, 2006; Chifflet, Torriglia, Chiesa, & Tolosa, 1988).

Unless otherwise stated, test compounds and drugs were purchased from Sigma-Aldrich (St. Louis, MO), American Radiolabeled Chemicals (St. Louis, MO), Tocris Bioscience (Ellisville, MO), or MedKoo Biosciences (Chapel Hill, NC). [^{3}H]Digoxin (40 Ci/mmol) was purchased from Perkin Elmer Life Sciences (Boston, MA).

LLC-PK1 cells (controls) and LLC-PK1 cells expressing a cDNA encoding human MDR1 Pgp (LLC-MDR1) were obtained from the Netherlands Cancer Institute (Amsterdam). The cells were maintained in Medium 199 supplemented with 10% fetal bovine serum, 2 mM L-glutamine, penicillin (50 units/mL) and streptomycin (50 μg/mL). Cells were maintained at 37°C in an atmosphere of 95% air/5% CO_2 and 90% relative humidity.

2.2 Purification and reconstitution of Pgp

Protein was determined by the method of Bradford (Bradford, 1976). Purified Pgp was reconstituted into proteoliposomes of egg phosphatidylcholine (Avanti Polar Lipids, Alabaster, AL) at a lipid:protein ratio of ~10:1 (w/w) using detergent removal by Sephadex G50 gel filtration chromatography (Romsicki & Sharom, 2001). Proteoliposomes were stored in aliquots at −80°C in HEPES buffer (20 mM HEPES, 100 mM NaCl, 5 mM $MgCl_2$, pH 7.4) containing 2 mM dithioerythritol.

2.3 Measurement of drug binding affinity of Pgp

The drug (test compound) binding affinity of Pgp in CHAPS micelles was measured using either saturable quenching of the intrinsic Trp fluorescence of the protein (Liu, Siemiarczuk,

& Sharom, 2000), or saturable quenching of 2-(4-maleimidoanilino)naphthalene-6-sulfonic acid (MIANS)-labeled Pgp (Liu & Sharom, 1996). Fluorescence titration data were fitted to an equation describing binding to a single site, and the dissociation constant, K_d, for binding of drug was estimated. No binding curves were obviously biphasic, and all fitted well to a single site model.

2.4 Fluorosome-trans-pgp production

Fluorosome-*trans*-pgp (Fl-*t*-pgp) was manufactured by the extrusion of purified reconstituted Pgp in HEPES buffer in the presence of bovine serum albumin (BSA)-fluorescein (Molecular Probes, Eugene, OR), resulting in unilamellar vesicles of ~200 nm diameter. Non-encapsulated BSA-fluorescein was removed by ultracentrifugation and Sepharose 6B gel-exclusion chromatography. Fl-*t*-pgp reagent consists of Fl-*t*-pgp in HEPES buffer (1 mg/mL) pre-incubated for a minimum of 5 min with 0.5 μM of the model transport substrate S-HR (The Fluorosome Company, Worcester, MA).

2.5 Fluorosome-trans-pgp assay

Liquid handling employed a Solo High-Throughput Single Channel Pipettor (Hudson Robotics, Springfield, NJ). Fl-*t*-pgp reagent (98 μL per well) was aliquoted into 96-well, half-well fluorescence microplates, and the plate was loaded into a NOVOStar microplate reader (BMG LABTECH, Durham, NC). Measurements were made at 23°C in well mode with fluorescence excitation at 480 nm and emission monitored at 520 nm. For each well, fluorescence was initially measured for 20 s to establish a baseline, then the Pgp pump was activated by rapidly injecting 5 μL of a stock solution of ATP in HEPES buffer using the NOVOStar onboard micropipettor, resulting in a final ATP concentration of 2 mM. The injection resulted in an immediate downward drop in fluorescence, which is an instrumental injection artifact (Jarrett Cheek, BMG LABTECH, personal communication). Fluorescence was monitored for an additional 40 s, with Pgp transport activity taken as the slope from 10–40 s after ATP injection. A flat baseline was observed when ATP was injected in the presence of 300 μM of the ATPase inhibitor sodium orthovanadate or when the non-hydrolyzable ATP analog adenosine 5′-(β,γ-imido)triphosphate (AMP-PNP, 2 mM final concentration) was injected, after the immediate artifactual drop in fluorescence.

2.6 Fluorosome-trans-pgp inhibition measurements

Inhibition measurements were made by adding 2 μL aliquots of test compound (drug) solutions in DMSO to 98 μL aliquots of Fl-*t*-pgp reagent in the wells of 96-well, half-well fluorescence microplates. Reference (control) wells had 2 μL of DMSO added to them. The microplates were shaken to ensure thorough mixing, and, after 5 min to establish equilibrium, the plate was loaded into the NOVOStar microplate reader. Fluorescence acquisition and initiation of transport were done as described above. All transport inhibition experiments were carried out at least twice. Slopes were calculated using BMG's onboard Mars software, and IC_{50} values were calculated using Prism Software (Graphpad Software, San Diego, CA) by fitting the Pgp transport activity (slope) at each test compound concentration to a robust fit for a one-phase decay. The IC_{50} value was calculated from this fit as that drug concentration causing 50% inhibition of Pgp transport activity. Similar results were obtained when the assay was performed in 384-well plates using starting volumes of 20–50 μL.

2.7 LLC-MDR1 inhibition measurements

Measurements were made as described previously (Reitman et al., 2011). Briefly, the LLC-MDR1 and control cell lines were cultured in 24-well trans-well culture plates (Millipore, Billerica, MA). [^{3}H]Digoxin (0.1 μM) and inhibitors were prepared in transport buffer

(Hanks buffer with 10 mM HEPES, pH 7.4). Prior to the transport study, cells were washed three times with transport buffer. [^{3}H]Digoxin substrate solution (500 μL) was added to either the apical (A) or basolateral (B) compartment of the culture plate, and buffer (500 μL) was added to the opposite compartment. Inhibitor (test compound) was added to both compartments. After 3 h incubation at 37°C, 50 μL samples were taken from both sides, and 200 μL of scintillant was added. Radioactivity was determined by liquid scintillation counting in a MicroBeta Trilux scintillation counter (Perkin Elmer; Boston, MA). All experiments were performed in triplicate.

Percentage of transport was calculated by dividing the concentration of digoxin measured in the receiver compartment by the sum of the concentrations measured in the receiver and donor compartments. Net transport of digoxin in LLC-MDR1 cells was calculated according to equation 1:

$$\text{Net transport} = (\%\ \text{transport B} \rightarrow \text{A}) - (\%\ \text{transport A} \rightarrow \text{B}) \quad (1)$$

Percent control transport in the presence of an inhibitor was calculated according to equation 2:

$$\%\ \text{control} = (R_I / R_o) \times 100 \quad (2)$$

where R_I represents net transport of digoxin measured in the presence of various concentrations of inhibitor, and R_o represents the net transport of digoxin in the absence of inhibitor.

IC_{50} values for inhibition of Pgp-mediated [^{3}H]digoxin transport were obtained by fitting the data to equation 3 by nonlinear regression analysis using Kaleidagraph software (KaleidaGraph Synergy Software, Reading, PA):

$$\%\ \text{control} = 100/(1 + I^s / IC_{50}{}^s) \quad (3)$$

where I is the inhibitor concentration (μM) and s is the Hill slope.

2.8 Statistics

Correlations between data sets were calculated using Prism assuming Gaussian (Pearson) populations.

3. Results

3.1 Preparation and characterization of Fluorosome-trans-pgp

The introduction of new technology makes it possible to quantitate the interaction of Pgp with its substrates in a fully defined *in vitro* system. Fl-*t*-pgp consists of synthetic unilamellar lipid vesicles manufactured as described in the Materials and methods. The Fl-*t*-pgp bilayer membrane is composed of egg phosphatidylcholine and contains highly purified functional Pgp (Liu, Siemiarczuk, & Sharom, 2000), reconstituted such that its ability to transport substrates is retained (Lu, Liu, & Sharom, 2001). Purified Pgp had high levels of ATPase activity (~1 μmol/min/mg) and previous work indicated that, following reconstitution, the protein displayed >40% of the drug transport activity it possessed in the native membrane vesicles from which it was purified (18). A single Fluorosome particle contains approximately 1,700 Pgp molecules, about half of which are expected to be oriented in an inside-out direction, with their nucleotide binding domains accessible on the outer surface of the lipid vesicle (Romsicki & Sharom, 1997). The Fl-*t*-pgp study described here utilized the Pgp model substrate S-HR, which has a K_d of 0.27 μM for binding to Pgp

and interacts with both the H and R sites of the transporter. The latter properties are consistent with the compound's IC_{50} values of 0.9 μM for H33342 transport (H-site) and 0.7 μM for tetramethylrosamine transport (R-site) (B. Vinepal and F.J. Sharom, unpublished data). The aqueous interior of the Fl-*t*-pgp particle contains the fluorescent sensor BSA-fluorescein. In solution, BSA-fluorescein binds S-HR, with a resulting change in fluorescein emission intensity, apparently due to a combination of static and dynamic fluorescence probe/substrate interactions, as indicated by life-time fluorescence studies (The Fluorosome Company, unpublished results).

The principle of operation of the Fl-*t*-pgp assay is illustrated in Fig. 1. Prior to the actual assay, the Pgp probe substrate S-HR is introduced into a preparation of Fl-*t*-pgp and passively diffuses through the Fl-*t*-pgp membrane to reach a state of equilibrium. Upon entering the aqueous interior of the Fl-*t*-pgp particle, the probe substrate rapidly binds to the fluorescent sensor, resulting in a new and stable fluorescence baseline (not shown). For a measurement, this "Fl-*t*-pgp reagent", aliquoted into the wells of a microplate, is placed in a fluorescence plate reader and the measurement initiated (step 1). After 20 s to ensure a stable baseline, ATP is injected (step 2). Substrate is then actively pumped by Pgp into the interior of the Fl-*t*-pgp particle, and the influxed substrate is rapidly bound by encapsulated sensor (step 3), resulting in a linear, time-dependent alteration of the fluorescence intensity (step 4). The screenshot in Fig. 2 demonstrates the result of a typical assay in the absence and presence of varying concentrations of the Pgp inhibitor cyclosporin A.

The added ATP activates only those Pgp molecules with their nucleotide binding sites facing the external solution. Proteins with the opposite orientation are non-functional in terms of transport, because the bilayer membrane is impermeable to ATP. Hydrolysis of ATP results in the active pumping of S-HR into the aqueous interior of the Fl-*t*-pgp particle, with concomitant changes in the fluorescence intensity of the sensor encapsulated in the vesicle lumen. No change in sensor fluorescence was observed in the presence of ATP together with the ATPase inhibitor orthovanadate, or when the non-hydrolyzable analog AMP-PNP was used, confirming that transport was driven by ATP hydrolysis. Thus the change in fluorescence emission intensity of the sensor with time is a direct monitor of the rate of Pgp transport of S-HR. Fl-*t*-pgp suspensions containing inhibitors in the absence of the substrate S-HR gave no time-dependent changes in fluorescence upon injection of ATP. Substrate transport by Fl-*t*-pgp has the important advantage that the only transporter present is Pgp, whereas additional drug transporters are expressed endogenously in the plasma membrane of cultured cells.

3.2 Inhibition of Pgp-mediated drug transport by Fluorosome-trans-pgp

Fl-*t*-pgp provides a direct measurement of Pgp activity in the presence of test compounds, thus allowing the direct determination of percent inhibition at any concentration of test compound, and IC_{50} values by measuring inhibition at varying concentrations of test compound. An example of real-time experimental determination of inhibition of Pgp activity by a drug is presented in Fig. 2, which shows the time course of ATP-dependent fluorescence emission by Fl-*t*-pgp reagent in the absence and presence of several concentrations of cyclosporin A, an established inhibitor of Pgp. The ratio of the slope for a kinetic run containing cyclosporin A to the slope of a run in its absence (control) gives the fractional reduction in Pgp transport activity at that concentration of cyclosporin A. Changes in fluorescence due to interaction of test compounds with the sensor are negligible and do not contribute to the observed slope.

The reproducibility of IC_{50} values obtained by the Fl-*t*-pgp technique is exemplified by 7 experiments with cyclosporin A carried out over a period of 14 months using three different

types of fluorescence plate readers; the average IC_{50} value was 0.58 μM with a standard error of 0.06 μM (10 %).

When test compounds are added to the Fl-*t*-pgp reagent before the injection of ATP, Pgp inhibitors reduce the rate of ATP-dependent transport of the substrate into the interior of the Fl-*t*-pgp particle, seen as a decrease in the rate of change (slope) of the fluorescence signal. In this way, IC_{50} values for inhibition of S-HR transport by Fl-*t*-pgp were determined for 46 test compounds (Table 1). The test compounds were drugs and drug candidates representing numerous therapeutic areas (anticancer drugs, HIV protease inhibitors, peptides, statins, β-blockers, ACE inhibitors, antidepressants, antifungal agents, anti-parasitic agents, calcium channel blockers, and anti-gout medications). Their IC_{50} values cover a range of over three orders of magnitude, and representative inhibition plots for 6 of these compounds with IC_{50} values ranging from 0.1 μM to 516 μM are shown in Fig. 3. It should be noted that those compounds developed as Pgp inhibitors, e.g. tariquidar, elacridar, valspodar, zosuquidar, show very low IC_{50} values, as does the classic Pgp inhibitor cyclosporin A. Among the less potent inhibitors is digoxin, a common substrate for cell-based assays (see also below), and its corresponding aglycone, digoxigenin.

3.3 Relationship between transport inhibition and binding affinity to Pgp

Substrate transport by Pgp is a complex multistep process (Callaghan, Ford, & Kerr, 2006), and details of the kinetics of the various steps involved remain elusive. Because an inhibitor (test compound) may compete with substrate for binding to Pgp in order to inhibit its transport and may itself be transported, the affinity of Pgp for binding a particular test compound should be closely related to its measured IC_{50} value for inhibition of substrate transport. To explore this relationship, Pgp binding affinities were determined using previously established fluorescence approaches. For example, test compound binding to purified Pgp in CHAPS micelles in solution leads to saturable quenching of the protein's intrinsic Trp fluorescence (Liu, Siemiarczuk, & Sharom, 2000), or quenching of an extrinsic fluorescent probe (MIANS) covalently linked to the protein via a cysteine residue (Liu & Sharom, 1996). Of the 46 compounds tested with Fl-*t*-pgp, K_d values were obtained for 33; these values are listed in Table 1. The remaining compounds were either autofluorescent and thus interfered with the assay, or did not produce high enough maximal quenching for accurate K_d estimation. A log-log plot of Fl-*t*-pgp IC_{50} values vs. Pgp K_d values for the corresponding compounds is shown in Fig. 4. The correlation (r^2) was 0.80. This suggests that the ability of a test compound to inhibit Pgp-mediated transport of substrate is indeed in general related to its binding affinity. It should be noted that this correlation extends over four orders of magnitude, from IC_{50} values in the nM range (tariquidar, 21 nM) to the mM range (digoxigenin, 0.52 mM). A few compounds (zosuquidar, paclitaxel) have an IC_{50} value substantially higher than the K_d value, however, other compounds have an IC_{50} value substantially lower than the K_d value, e.g. nicardipine, nifedipine, elacridar. It is not easy to explain these differences for individual test drugs, especially since the mechanisms by which they inhibit Pgp are unknown. The different assay systems used to measure IC_{50} and K_d (liposomes vs. purified protein in detergent solution) may account for the less than perfect correlation between the two parameters.

3.4 Inhibition of Pgp-mediated drug transport in LLC-MDR1 cell monolayers

In order to compare inhibition data from the Fl-*t*-pgp system with those from an intact cell assay system, cultured monolayers of LLC-MDR1 cells expressing recombinant Pgp were used to assess inhibition of [^{3}H]digoxin transport by a subset of 16 of the test compounds previously tested with Fl-*t*-pgp. Transport of digoxin was determined in the B→A and A→B directions as described in Materials and methods, and the net transport was calculated in the absence and presence of various concentrations of the 16 test compounds. Representative

plots of inhibition of [^{3}H]digoxin transport by two test compounds are shown in Fig. 5, and IC_{50} values calculated from the net transport values are presented in Table 1. In general, the results of the cell-based assay parallel those derived from Fl-*t*-pgp. A log-log plot of cell-based IC_{50} values with those derived from Fl-*t*-pgp is shown in Fig. 6. The data sets have a correlation (r^2) of 0.994. The IC_{50} values measured in LLC-MDR1 cells were systematically higher than those measured using the Fl-*t*-Pgp system (Table 1). This trend may be caused by the differences between an *in vitro* vesicle-based system and a cell-based system, or they could arise from differences in drug interactions or the mechanism of inhibition between rodent and human Pgp. Since the trend is systematic, it seems more likely that it arises from the first possibility. Intact cell systems have an inherent tendency to adsorb or bind drugs non-specifically, which would lower the amount of drug available to interact with Pgp, thus requiring a higher concentration to observe inhibition.

3.5 Correlation of Fluorosome-trans-pgp results with digoxin-drug interaction data

Further investigation of the Fl-*t*-pgp inhibition assay was carried out by correlating IC_{50} values with *in vivo* data for the effects of various co-administered second drugs ("inhibitors") on the area under the curve (AUC) after oral administration and maximum plasma levels at steady state ($C_{max,ss}$) of digoxin in human patients. Relevant data for digoxin, AUC and AUC_I and $C_{max,ss}$ and $C_{max,ss,I}$, in the absence and presence of inhibitor I, respectively, were taken from Fenner et al. (Fenner et al., 2009). [I] is the published peak plasma concentration of drug (inhibitor) I, and [I_2] is the estimated intestinal concentration of drug (inhibitor) I (compiled in Fenner et al., 2009). The ratios AUC_I/AUC and $C_{max,ss,I}$ / $C_{max,ss}$ represent the effect of drug (inhibitor) on exposure to digoxin in humans. It has been assumed that a change in digoxin exposure of >25%, i.e. AUC_I/AUC and $C_{max,ss,I}/C_{max,ss}$ >1.25, would represent a potentially toxic effect caused by the second drug (inhibitor), and values of [I]/IC_{50} > 0.1 and [I_2]/IC_{50} > 10 have been set as cutoffs for significant changes in digoxin disposition (Giacomini et al., 2010). $IC_{50,Fl}$ values are half-maximal inhibitory concentrations of drugs from Fl-*t*-pgp assays (Table 2). Table 2 summarizes the data used in the correlations.

Plots of AUC_I/AUC and $C_{max,ss,I}/C_{max,ss}$ vs. I/IC_{50} and I_2/IC_{50}, where IC_{50} are values measured with Fl-*t*-pgp, are shown in Figs. 7a–d. In all cases, compounds in the upper left quadrant are "false negatives" and those in the lower right quadrant are "false positives". Using the IC_{50} values measured with Fl-*t*-pgp for 16 of the 19 drugs reported by Fenner et al. (Fenner et al., 2009), the resulting plots are at least equivalent, if not superior, to those based on inhibition of net secretory flux in Caco-2 cell monolayers reported in that paper. In particular, the plot of AUC_I/AUC vs. [I_2]/IC_{50} (Fig. 7b) leaves a single false negative (captopril), and the plot of $C_{max,ss,I}/C_{max,ss}$ against [I_2]/IC_{50} (Fig. 7d) leaves two false negatives (captopril and felodipine). Fewer false positives are seen in both correlations with [I]/IC_{50} (Figs. 7a and 7c) compared with those of Fenner et al. (Fenner et al., 2009).

4. Discussion

In this work, we report the preparation of a novel reagent, and demonstrate its utility as an *in vitro* method to screen drugs and other test compounds for inhibition of the important drug efflux transporter Pgp. Incorporation of purified mammalian Pgp into a lipid bilayer vesicle containing a fluorescent sensor in the aqueous interior - Fl-*t*-pgp - affords a specific assay for measuring interaction of test compounds with the transporter in real time. The Fl-t-pgp reagent makes use of rodent (hamster) Pgp rather than human Pgp, because extensive studies of the former protein over many years have indicated that it has high ATPase and drug transport activity, and is sufficiently robust for development of such an assay reagent. In contrast, purified human Pgp proved to be too unstable for production of a reconstituted vesicle system that can maintain drug transport function over a period of several days (F.J.

Sharom, unpublished data). It should be noted that the recent crystal structure of Pgp was determined using the mouse protein (Aller et al., 2009) for similar reasons. Hamster Pgp (Abcb1a) is very closely related to the human protein, with 87% amino acid sequence identity and 93% similarity. Indeed, the transmembrane regions of the two proteins where the drug-binding pocket is located show an even greater degree of similarity/identity and the important residues involved in substrate binding are highly conserved (Aller et al., 2009). Species differences in drug transport specificity between rodent and human Pgp observed in cell-based assays are small, and may be artifacts arising from assay format, different expression levels and transport substrates (Booth-Genthe et al., 2006; Zolnerciks, Booth-Genthe, Gupta, Harris, & Unadkat, 2011), as well as differences in expression of other drug transporters (Acharya et al., 2008). When 3300 Pfizer compounds were tested in human MDR1-MDCK and mouse Mdr1a-MDCK trans-well assays, a very good correlation was observed ($R^2 = 0.92$) between the efflux ratios in MDR1-MDCK and Mdr1a-MDCK cells (Feng et al., 2008). This group concluded that mouse Pgp is a useful model to predict human Pgp activity *in vivo*. The ABCB1-transfected cell lines currently used for identification of Pgp substrates are also not ideal models, because the activity and specificity of Pgp may vary with expression level and host cell type. Human Pgp in different tissues (e.g. intestine vs. blood brain barrier) may also display variations in activity and specificity, so that exactly mimicking the *in vivo* situation in an *in vitro* assay system is not possible.

Compounds that interact with Pgp may be substrates and/or inhibitors. The Fl-*t*-pgp assay identifies both types of compounds without distinction, because it is based on competition/inhibition of transport of a probe substrate. It is still not clear how Pgp inhibitors act at the molecular level. Some of these compounds (e.g. verapamil, cyclosporin A) are themselves transported, and clearly compete with substrates for binding to Pgp (reviewed in Sharom, 1997). However, others (e.g. zosuquidar/LY335979) display prolonged high affinity binding to the protein (Starling et al., 1997), suggesting that some inhibitors block transport by interacting very tightly with the substrate binding pocket of Pgp. The recent X-ray crystal structure of Pgp (Aller et al., 2009), as well as several biochemical studies (Loo, Bartlett, & Clarke, 2003; Lugo & Sharom, 2005), indicate that the protein contains a large flexible multi-site binding pocket that can accommodate at least two drug molecules simultaneously in distinct sub-sites. It was shown earlier that two major functional transport sub-sites exist; one (the H-site) transports Hoechst 33342 (bisbenzimide), the other (the R-site) transports the fluorescent dye, rhodamine 123 (Shapiro & Ling, 1997). Steric and allosteric interactions between these sub-sites result in one drug having either stimulatory or inhibitory effects on transport of a second drug, and led to the proposal of a complex interaction network between them (Martin et al., 2000). How interactions between drugs at the level of transport are related to the structure of the Pgp binding pocket in molecular terms is not well understood. However, the location of two pseudo-symmetric translocation pathways through the protein has recently been reported (Parveen et al., 2011). The complication of multiple binding sites and the interactions between them has not really been addressed in cell-based assays for Pgp substrates and inhibitors (Zolnerciks, Booth-Genthe, Gupta, Harris, & Unadkat, 2011), and may require the use of several reference compounds, which is not practical where many drugs are to be tested. The Fl-*t*-pgp system lends itself to mechanistic studies of Pgp function. By varying the concentration of substrate as well as inhibitor, K_i values for different drugs as well as the type of inhibition, e.g. competitive or non-competitive, can be investigated. This may shed further light on the clearly complex relationship between drug binding sub-sites.

Evidence that the Fl-*t*-pgp system is a true mimic of the transporter in cell membranes is afforded by the described results, which show that: 1) the assay responds to ATP, producing a linear change in fluorescence consistent with transport of the substrate S-HR (Fig. 2); 2) transport of the substrate depends on ATP hydrolysis; 3) IC_{50} values of test compounds

correlated well with K_d, i.e. the binding affinity of the transporter for these compounds (Fig. 4); and 4) IC_{50} values of test compounds are in a similar rank order and comparable in magnitude to those obtained by a conventional, cell-based method for a subset of the test compounds (Table 1). It should be noted that the transport substrate S-HR used with the Fl-*t*-pgp system is able to interact with both the H-site and R-site of Pgp (B. Vinepal and F.J. Sharom, unpublished data). This provides an advantage over other reference substrates, which in many cases have not been characterized for interactions with these sites.

There are several cell-based and vesicle-based methods currently in use to determine substrate and/or inhibitor properties of test compounds on Pgp (Sharom & Siarheyeva, 2008). These include monolayers of Caco-2 cells, which express native Pgp, other cell lines stably transfected with human Pgp cDNA (LLC-MDR1 and MDCK-MDR1), and inside-out membrane vesicles isolated from cell lines expressing recombinant human Pgp. Various reference substrates, e.g. [^{3}H]digoxin (which interacts poorly with Pgp, with high K_d and IC_{50} values, see Table 1) or other radiolabeled compounds are used, often at different concentrations. The lack of agreement between results obtained using different cell-based systems, as well as between results obtained using the same system in different laboratories (see below), as well as variations in mathematical processing of assay data, create uncertainty in the validity of these results. The requirement for sterile conditions to maintain and grow cells, the cumbersome and time-consuming assay conditions, and the need for acquiring and handling of radioactive substrates, further complicate the use of cell-based methodologies.

The wide variation in reported IC_{50} values for Pgp inhibitors is a confounding factor in interpretation of drug-drug interaction data. A review of published results on several of these compounds (designated by the International Transporter Consortium to be employed as "selected inhibitors" of Pgp; see Giacomini et al., 2010), obtained using a variety of cell- and vesicle-based assays and employing various test substrates, reveals the following variations in IC_{50} values: tariquidar, 60.5-fold (Weiss & Haefeli, 2006; Klinkhammer, Muller, Globisch, Pajeva, & Wiese, 2009; Höcheri, 2010; Dickens, Owen, Alfirevic, & Pirmohamed, 2009), cyclosporin A, 12.4-fold (Klinkhammer, Muller, Globisch, Pajeva, & Wiese, 2009; Dickens et al., 2009; Rautio et al., 2006; U.S.Department of Health and Human Services Food and Drug Administration (FDA), 2006), quinidine hydrochloride, 25.2-fold (Weiss & Haefeli, 2006; Rautio et al., 2006; U.S.Department of Health and Human Services Food and Drug Administration (FDA), 2006; Fenner et al., 2009), and verapamil, 29-fold (Weiss & Haefeli, 2006; Klinkhammer, Muller, Globisch, Pajeva, & Wiese, 2009; Dickens et al., 2009; Rautio et al., 2006; U.S.Department of Health and Human Services Food and Drug Administration (FDA), 2006; Fenner et al., 2009) (see also Lee, 2011). The significant variations in IC_{50} values underscore the need for simple and robust assays to give accurate inhibitor information for Pgp (and related transporters). With additional studies, the Fl-*t*-pgp assay described in this work may prove to be valuable in this regard.

The ultimate test of an assay is whether its results accurately correlate with real properties of drugs in human patients. Fenner and co-workers (Fenner et al., 2009) provided a novel approach to this problem by correlating published effects of drugs on digoxin levels in human patients with parameters of their inhibition of Pgp. Our use of potencies of drugs (inhibitors) derived from Fl-*t*-pgp assays (Table 2) showed at least equivalent, if not superior, correlations with digoxin disposition (Figs. 7a–d). To make effective use of the IC_{50} values determined using the Fl-*t*-pgp assay, they will need to be compared to relevant drug exposure levels *in vivo*. For example, drug concentrations in the gut will be substantially higher than those in the plasma. The current guidance published by the

International Transporter Consortium indicates how to establish the clinical relevance of *in vitro* data of the type presented in this study (Giacomini et al., 2010).

5. Summary

We have created for the first time a transporter assay system that enables definitive measurement of Pgp activity and its inhibition in real time. We have demonstrated that for a large panel of test compounds (drugs) IC_{50} values resulting from this assay are consistent with their binding affinities to Pgp and are in agreement both with data from cell monolayer-based assays and published results of human drug-drug interaction studies using digoxin. Fl-*t*-pgp is the first of a series of drug transporter-lipid vesicle constructs that can be used for high-throughput screening of drugs and potential drug candidates, and for research into the mechanisms of substrate transport and drug-drug interactions. Since the studies described above, we have been able to employ the Fluorosome assay in 384-well microplates using a starting volume of Fl-*t*-pgp reagent as low as 20 μL, thereby decreasing the amount of test drug required to carry out the assay, and its concomitant cost. The Fluorosome platform is simple in application, offers fast turnover (40 s per data point; a 7-point IC50 can be determined in <6 min), gives real-time measurements with immediate results, and is fully amenable to robotics, allowing rapid throughput. It uses very small quantities of test drug, and since it employs minimal instrumentation, minimal labor and has no requirement for sterility, is a cost-effective approach relative to cell culture methodologies. The well defined nature of this platform also obviates many of the inherent complications and ambiguities inherent in cell-based systems.

Abbreviations

ABC	ATP-binding cassette
AMP-PNP	adenosine 5′-(β,γ-imido)triphosphate
AUC	area under the curve
BSA	bovine serum albumin
CHAPS	3-[(3-cholamidopropyl)-dimethylammonio]-1-propanesulfonate
Fl-*t*-pgp	Fluorosome-*trans*-pgp
MIANS	2-(4-maleimidoanilino)naphthalene-6-sulfonic acid
Pgp	P-glycoprotein (ABCB1, MDR1)

Acknowledgments

Funding for this study was provided by NIH grant R44 GM075397 (DLM) and the Canada Research Chairs program (FJS), and by the Merck New Technology Review and Licensing Committee. The authors would like to thank Jairam Palamanda and Mitchell Green for critically reading the manuscript.

References

Acharya P, O'Connor MP, Polli JW, Ayrton A, Ellens H, Bentz J. Kinetic identification of membrane transporters that assist P-glycoprotein-mediated transport of digoxin and loperamide through a confluent monolayer of MDCKII-hMDR1 cells. Drug Metabolism and Disposition: The Biological Fate of Chemicals. 2008; 36:452–460. [PubMed: 17967933]

Aller SG, Yu J, Ward A, Weng Y, Chittaboina S, Zhuo R, et al. Structure of P-glycoprotein reveals a molecular basis for poly-specific drug binding. Science. 2009; 323:1718–1722. [PubMed: 19325113]

Booth-Genthe CL, Louie SW, Carlini EJ, Li B, Leake BF, Eisenhandler R, et al. Development and characterization of LLC-PK1 cells containing Sprague-Dawley rat Abcb1a (Mdr1a): comparison of rat P-glycoprotein transport to human and mouse. Journal of Pharmacological and Toxicological Methods. 2006; 54:78–89. [PubMed: 16545584]

Bradford MM. A rapid and sensitive method for the quantitation of microgram quantities of protein utilizing the principle of protein-dye binding. Analytical Biochemistry. 1976; 72:248–254. [PubMed: 942051]

Callaghan R, Ford RC, Kerr ID. The translocation mechanism of P-glycoprotein. FEBS Letters. 2006; 580:1056–1063. [PubMed: 16380120]

Chifflet S, Torriglia A, Chiesa R, Tolosa S. A method for the determination of inorganic phosphate in the presence of labile organic phosphate and high concentrations of protein: application to lens ATPases. Analytical Biochemistry. 1988; 168:1–4. [PubMed: 2834977]

Dickens D, Owen A, Alfirevic A, Pirmohamed M. Determination of the inhibitory potencies of p-glycoprotein inhibitors by transcellular permeability of Caco-2 cells. Proceedings of the British Pharmacological Society. 2009 http://pa2online.org/abstracts/Vol7Issue4abst092P.pdf.

Eckford PD, Sharom FJ. P-glycoprotein (ABCB1) interacts directly with lipid-based anti-cancer drugs and platelet-activating factors. Biochemistry and Cell Biology. 2006; 84:1022–1033. [PubMed: 17215888]

Eckford PD, Sharom FJ. ABC efflux pump-based resistance to chemotherapy drugs. Chemical Reviews. 2009; 109:2989–3011. [PubMed: 19583429]

Feng B, Mills JB, Davidson RE, Mireles RJ, Janiszewski JS, Troutman MD, et al. In vitro P-glycoprotein assays to predict the in vivo interactions of P-glycoprotein with drugs in the central nervous system. Drug Metabolism and Disposition: The Biological Fate of Chemicals. 2008; 36:268–275. [PubMed: 17962372]

Fenner KS, Troutman MD, Kempshall S, Cook JA, Ware JA, Smith DA, et al. Drug-drug interactions mediated through P-glycoprotein: clinical relevance and in vitro-in vivo correlation using digoxin as a probe drug. Clinical Pharmacology and Therapeutics. 2009; 85:173–181. [PubMed: 18987624]

Giacomini KM, Huang SM, Tweedie DJ, Benet LZ, Brouwer KL, Chu X, et al. Membrane transporters in drug development. Nature Reviews in Drug Discovery. 2010; 9:215–236.

Höcheri, P. Ph.D. Dissertation. Universität Regensburg; 2010. New tariquidar-like ABCB1 modulators in cancer chemotherapy: Preclinical pharmacokinetic/pharmacodynamic investigations and computational studies.

Klinkhammer W, Muller H, Globisch C, Pajeva IK, Wiese M. Synthesis and biological evaluation of a small molecule library of 3rd generation multidrug resistance modulators. Bioorganic and Medicinal Chemistry. 2009; 17:2524–2535. [PubMed: 19250834]

Lee, CA. Assessment of P-glycoprotein inhibitory potency (IC_{50}) variability in various in vitro experimental systems. AAPS Workshop on Drug Transporters in ADME: from the Bench to the Bedside; Bethesda MD. 2011.

Leslie EM, Deeley RG, Cole SPC. Multidrug resistance proteins: role of P-glycoprotein, MRP1, MRP2, and BCRP (ABCG2) in tissue defense. Toxicology and Applied Pharmacology. 2005; 204:216–237. [PubMed: 15845415]

Liu R, Sharom FJ. Site-directed fluorescence labeling of P-glycoprotein on cysteine residues in the nucleotide binding domains. Biochemistry. 1996; 35:11865–11873. [PubMed: 8794769]

Liu R, Siemiarczuk A, Sharom FJ. Intrinsic fluorescence of the P-glycoprotein multidrug transporter: sensitivity of tryptophan residues to binding of drugs and nucleotides. Biochemistry. 2000; 39:14927–14938. [PubMed: 11101309]

Loo TW, Bartlett MC, Clarke DM. Simultaneous binding of two different drugs in the binding pocket of the human multidrug resistance P-glycoprotein. Journal of Biological Chemistry. 2003; 278:39706–39710. [PubMed: 12909621]

Lu P, Liu R, Sharom FJ. Drug transport by reconstituted P-glycoprotein in proteoliposomes. Effect of substrates and modulators, and dependence on bilayer phase state. European Journal of Biochemistry. 2001; 268:1687–1697. [PubMed: 11248688]

Lugo MR, Sharom FJ. Interaction of LDS-751 and rhodamine 123 with P-glycoprotein: evidence for simultaneous binding of both drugs. Biochemistry. 2005; 44:14020–14029. [PubMed: 16229491]

Martin C, Berridge G, Higgins CF, Mistry P, Charlton P, Callaghan R. Communication between multiple drug binding sites on P-glycoprotein. Molecular Pharmacology. 2000; 58:624–632. [PubMed: 10953057]

Parveen Z, Stockner T, Bentele C, Pferschy S, Kraupp M, Freissmuth M, et al. Molecular dissection of dual pseudosymmetric solute translocation pathways in human P-glycoprotein. Molecular Pharmacology. 2011; 79:443–452. [PubMed: 21177413]

Polli JW, Wring SA, Humphreys JE, Huang LY, Morgan JB, Webster LO, et al. Rational use of in vitro P-glycoprotein assays in drug discovery. Journal of Pharmacology and Experimental Therapeutics. 2001; 299:620–628. [PubMed: 11602674]

Rautio J, Humphreys JE, Webster LO, Balakrishnan A, Keogh JP, Kunta JR, et al. In vitro P-glycoprotein inhibition assays for assessment of clinical drug interaction potential of new drug candidates: A recommendation for probe substrates. Drug Metabolism and Disposition: The Biological Fate of Chemicals. 2006; 34:786–792. [PubMed: 16455806]

Reitman ML, Chu X, Cai X, Yabut J, Venkatasubramanian R, Zajic S, et al. Rifampin's acute inhibitory and chronic inductive drug interactions: experimental and model-based approaches to drug-drug interaction trial design. Clinical Pharmacology and Therapeutics. 2011; 89:234–242. [PubMed: 21191377]

Romsicki Y, Sharom FJ. Interaction of P-glycoprotein with defined phospholipid bilayers: a differential scanning calorimetric study. Biochemistry. 1997; 36:9807–9815. [PubMed: 9245413]

Romsicki Y, Sharom FJ. Phospholipid flippase activity of the reconstituted P-glycoprotein multidrug transporter. Biochemistry. 2001; 40:6937–6947. [PubMed: 11389609]

Schinkel AH. Pharmacological insights from P-glycoprotein knockout mice. International Journal of Clinical Pharmacology and Therapeutics. 1998; 36:9–13. [PubMed: 9476142]

Shapiro AB, Ling V. Positively cooperative sites for drug transport by P-glycoprotein with distinct drug specificities. European Journal of Biochemistry. 1997; 250:130–137. [PubMed: 9432000]

Sharom FJ. The P-glycoprotein efflux pump: how does it transport drugs? Journal of Membrane Biology. 1997; 160:161–175. [PubMed: 9425600]

Sharom FJ. ABC multidrug transporters: structure, function and role in chemoresistance. Pharmacogenomics. 2008; 9:105–127. [PubMed: 18154452]

Sharom, FJ.; Siarheyeva, A. Functional assays for identification of compounds that interact with P-gp. In: Colabufo, NA., editor. Multidrug Resistance: Biological and Pharmaceutical Advances in Antitumour Treatment. Trivandrum (India): Research Signpost; 2008. p. 261-290.

Starling JJ, Shepard RL, Cao J, Law KL, Norman BH, Kroin JS, et al. Pharmacological characterization of LY335979: a potent cyclopropyldibenzosuberane modulator of P-glycoprotein. Advances in Enzyme Regulation. 1997; 37:335–347. [PubMed: 9381979]

U.S. Department of Health and Human Services Food and Drug Administration (FDA). Guidance for industry: Drug interaction studies - study design, data analysis, and implications for dosing and labelling. [Electronic version]. 2006. Available from: http://www.fda.gov/downloads/Drugs/GuidanceComplianceRegulatoryInformation/Guidances/ucm072101.pdf

Weiss J, Haefeli WE. Evaluation of inhibitory potencies for compounds inhibiting P-glycoprotein but without maximum effects: f2 values. Drug Metabolism and Disposition: The Biological Fate of Chemicals. 2006; 34:203–207. [PubMed: 16272402]

Zolnerciks JK, Booth-Genthe CL, Gupta A, Harris J, Unadkat JD. Substrate- and species-dependent inhibition of P-glycoprotein-mediated transport: implications for predicting in vivo drug interactions. Journal of Pharmaceutical Sciences. 2011; 100:3055–3061. [PubMed: 21484807]

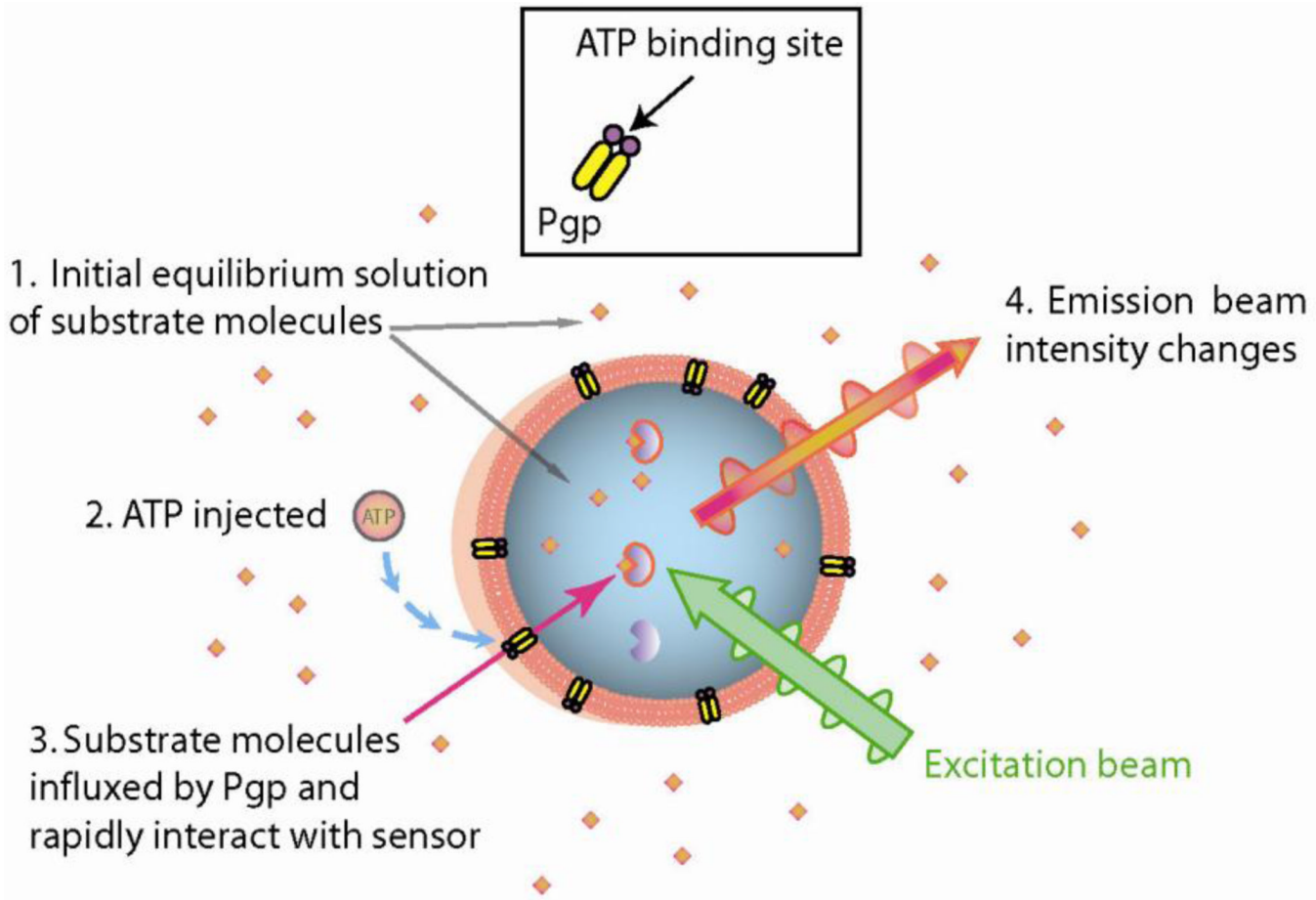

Fig. 1.

Fl-*t*-pgp principles of operation. Fl-t-pgp consists of purified Pgp reconstituted into the bilayers of unilamellar liposomes that contain drug-binding fluorescent sensor molecules in their aqueous interior. Prior to the actual assay, the Pgp substrate S-HR is introduced into a preparation of Fl-*t*-pgp and passively diffuses through the membrane to reach a state of equilibrium. Upon entering the aqueous interior of the Fl-*t*-pgp particle, the substrate rapidly binds to the fluorescent sensor, resulting in a new and stable fluorescence baseline (not shown). 1. To conduct a transport assay, “Fl-*t*-pgp reagent” in the wells of a microplate is placed in a fluorescence plate reader, and measurement is initiated. 2. ATP is injected. 3. Substrate is actively pumped by Pgp against a concentration gradient into the interior of the Fl-*t*-pgp particle, and the influxed substrate is rapidly bound by the encapsulated fluorescent sensor. 4. A linear, time-dependent alteration of the fluorescence intensity is observed.

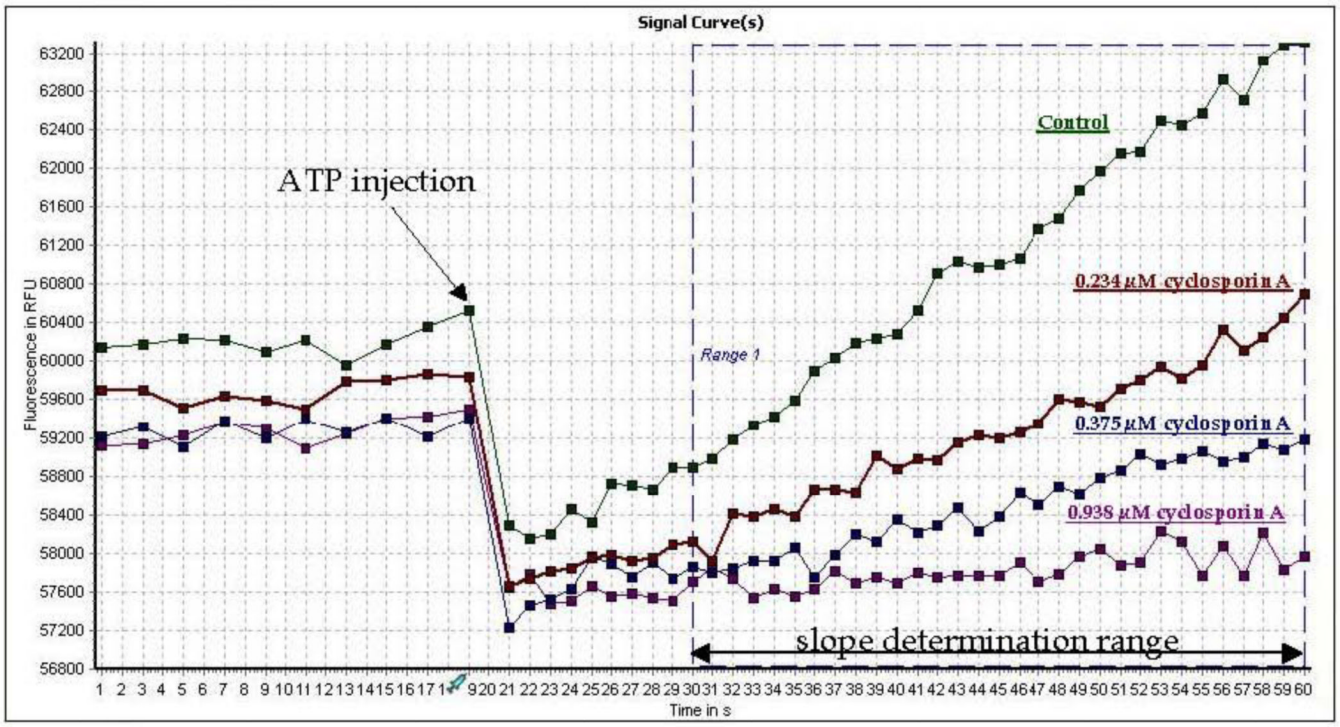

Fig. 2.

Screen shot of Pgp activity assay using Fl-*t*-pgp reagent in the presence of three concentrations of cyclosporin A. Samples (100 µL each) in a BMG NOVOStar injecting fluorescence plate reader were scanned in well mode for 20 s to establish a baseline. At 20 s, 5 µL of ATP stock solution was rapidly injected into each well (final concentration 2 mM), and fluorescence increase was monitored over 30 s, beginning 10 s post-injection. (The sharp drop in fluorescence observed upon ATP injection is an instrumental artifact.) Onboard software calculated the slope of fluorescence at each concentration of cyclosporin A, and % of Pgp inhibition at each concentration of cyclosporin A is the ratio of that slope to the control slope.

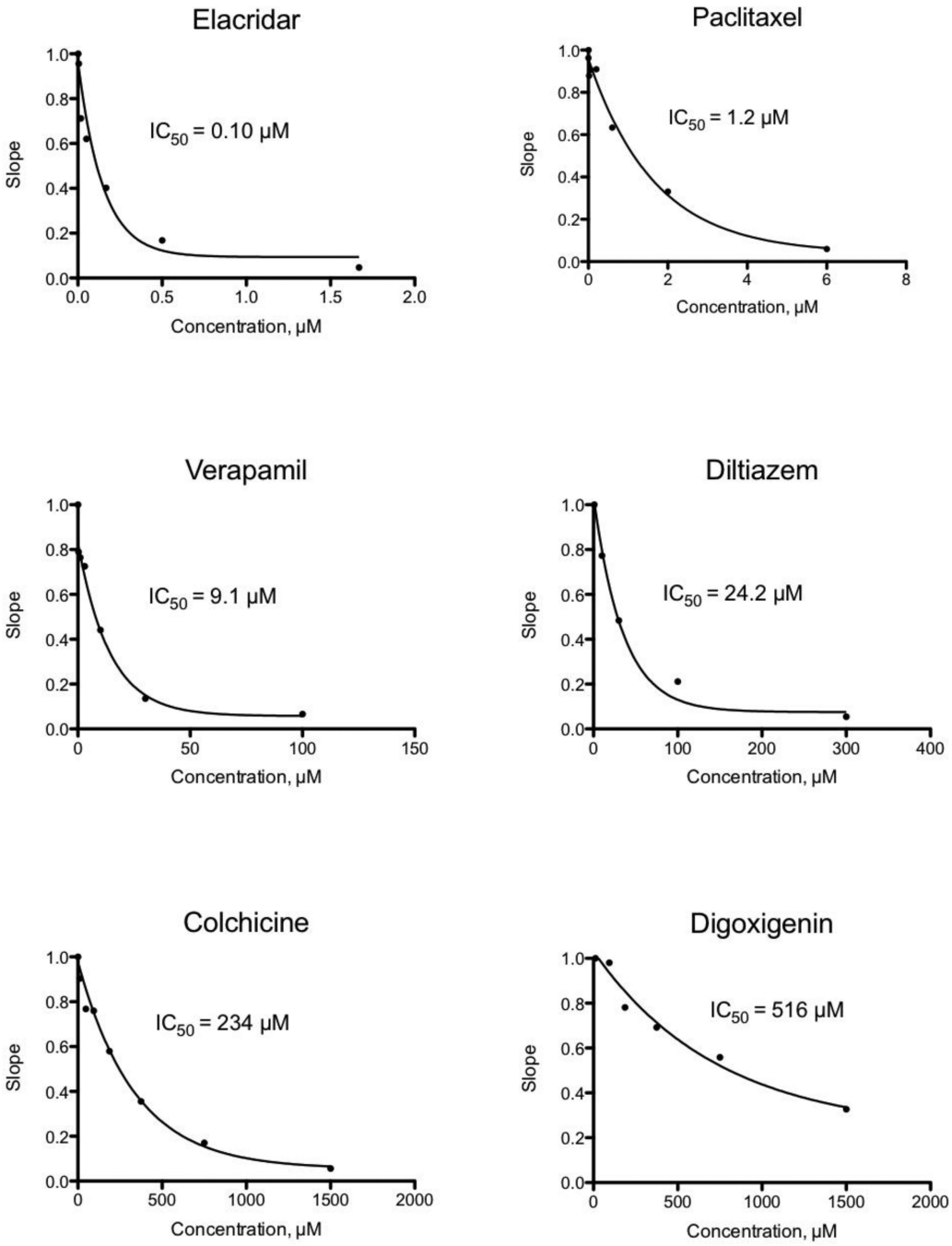

Fig. 3.

Representative IC_{50} plots derived from Fl-*t*-pgp assays. Individual points represent the activity of Pgp in the presence and absence of test compound, normalized to a value of 1 for controls. IC_{50} values were calculated by fitting the relative activity at each test compound concentration to a monophasic decay. The IC_{50} value is the test compound concentration causing 50% inhibition of Pgp transport activity.

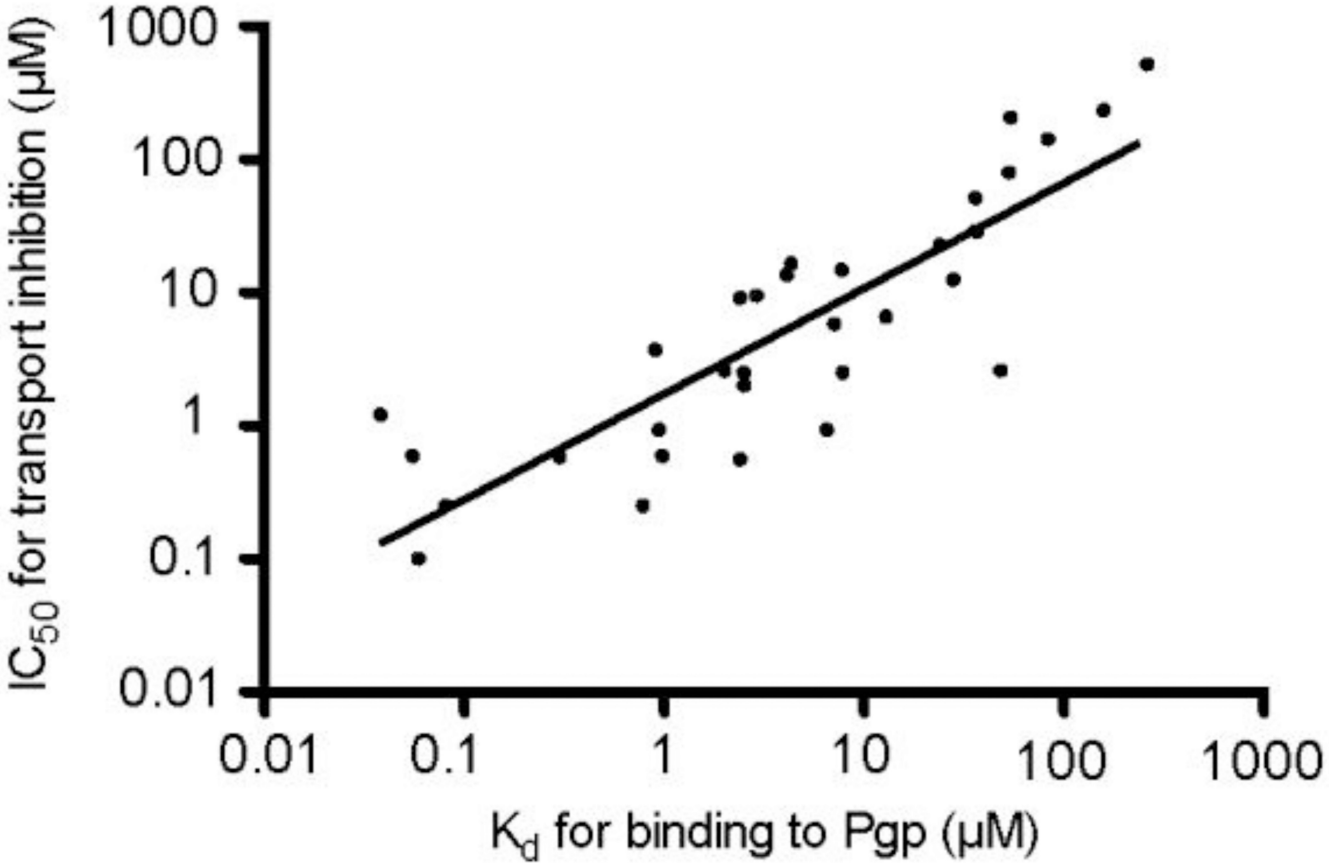

Fig. 4.

Plot (log-log) of the IC_{50} values for Pgp transport inhibition obtained with Fl-*t*-pgp and K_d values for Pgp binding for 33 test compounds. IC_{50} values for transport inhibition were determined using the Fl-*t*-pgp assay, and K_d values were determined by fluorescence quenching of purified Pgp in 2 mM CHAPS.

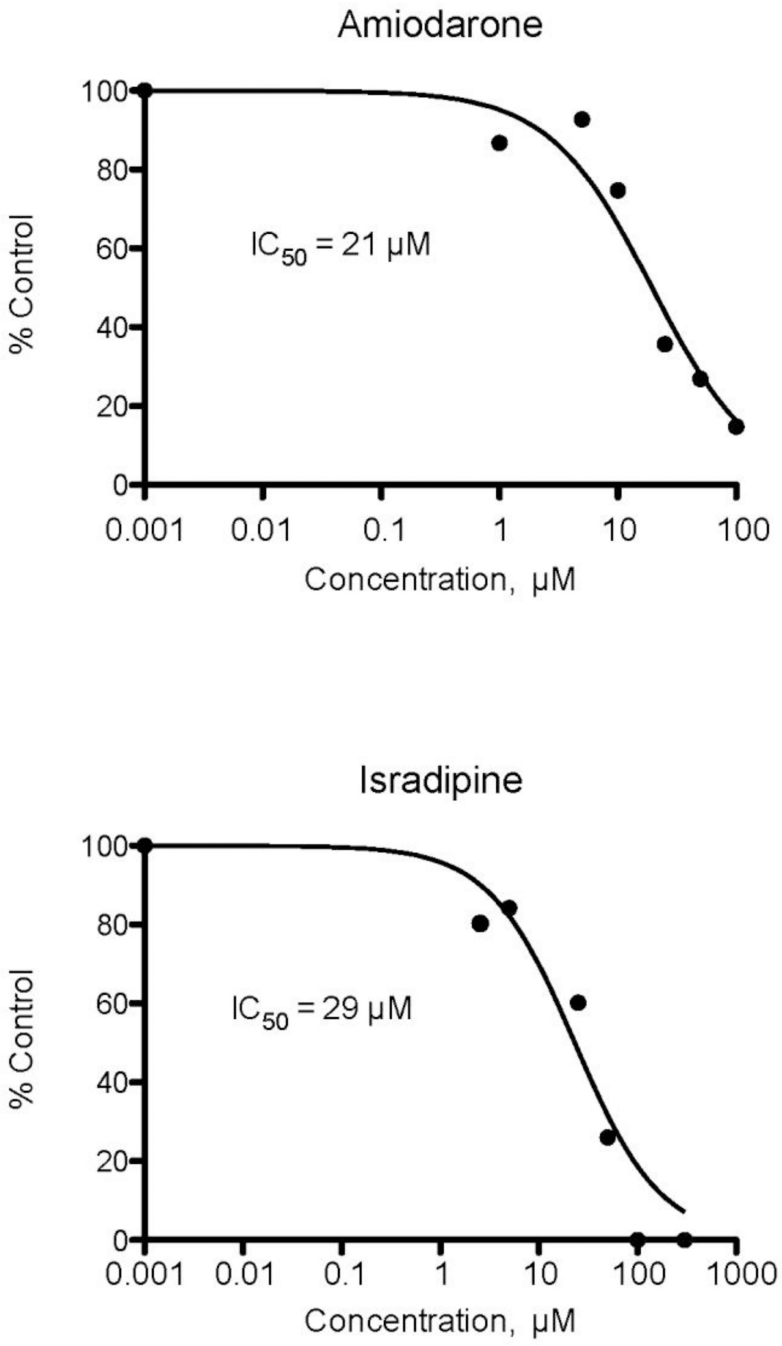

Fig. 5.

Representative IC_{50} plots derived from net transport measurements of [^{3}H]digoxin transport in LLC-MDR1 cell monolayers. Individual points represent the inhibition of Pgp-mediated digoxin transport at varying concentrations of test compounds. IC_{50} values were calculated by non-linear regression analysis as described in Materials and methods.

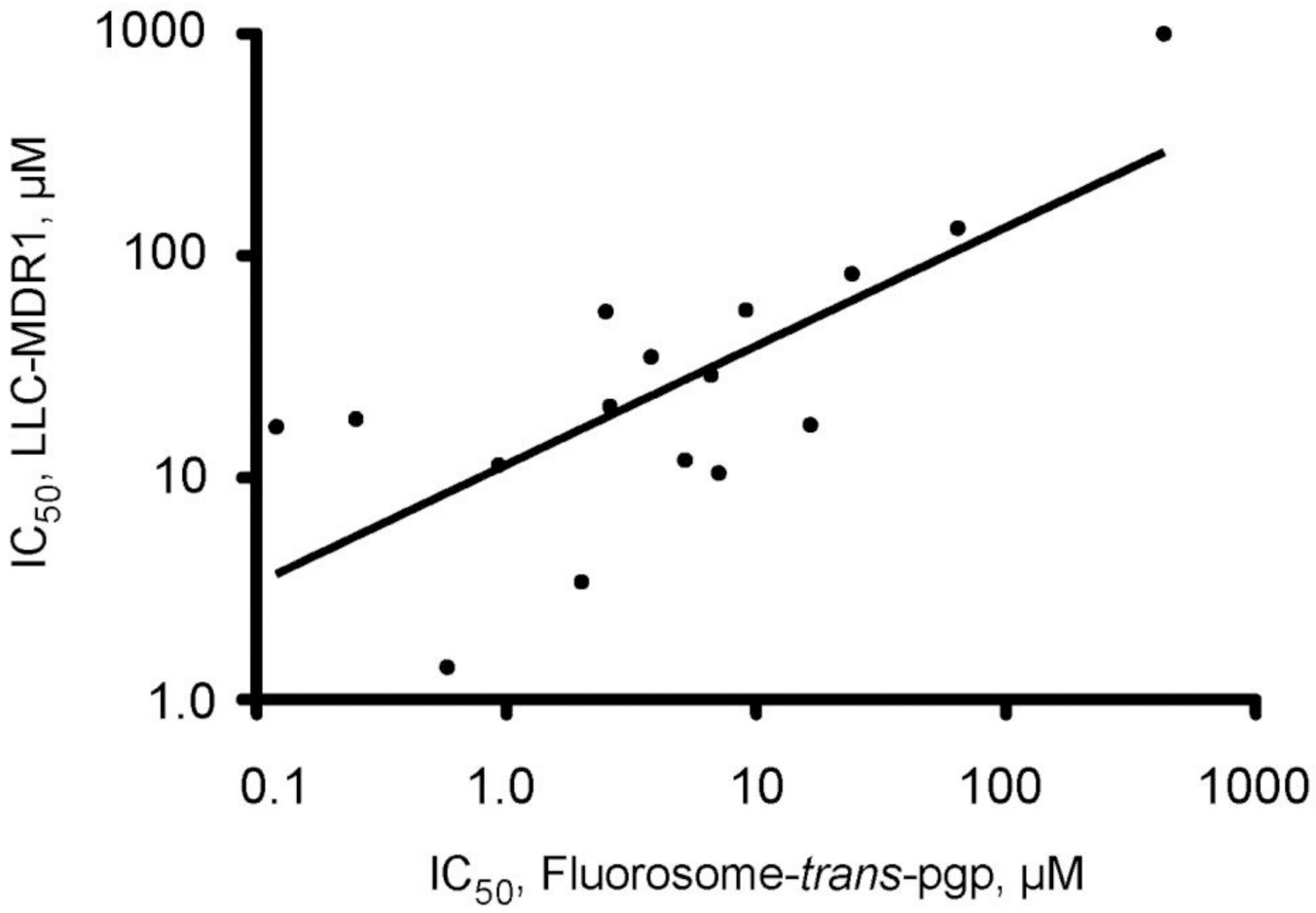

Fig. 6.

Plot (log-log) of the IC_{50} values for transport inhibition determined using LLC-MDR1 cell monolayers and IC_{50} values for transport inhibition determined using the Fl-*t*-pgp assay for 16 test compounds.

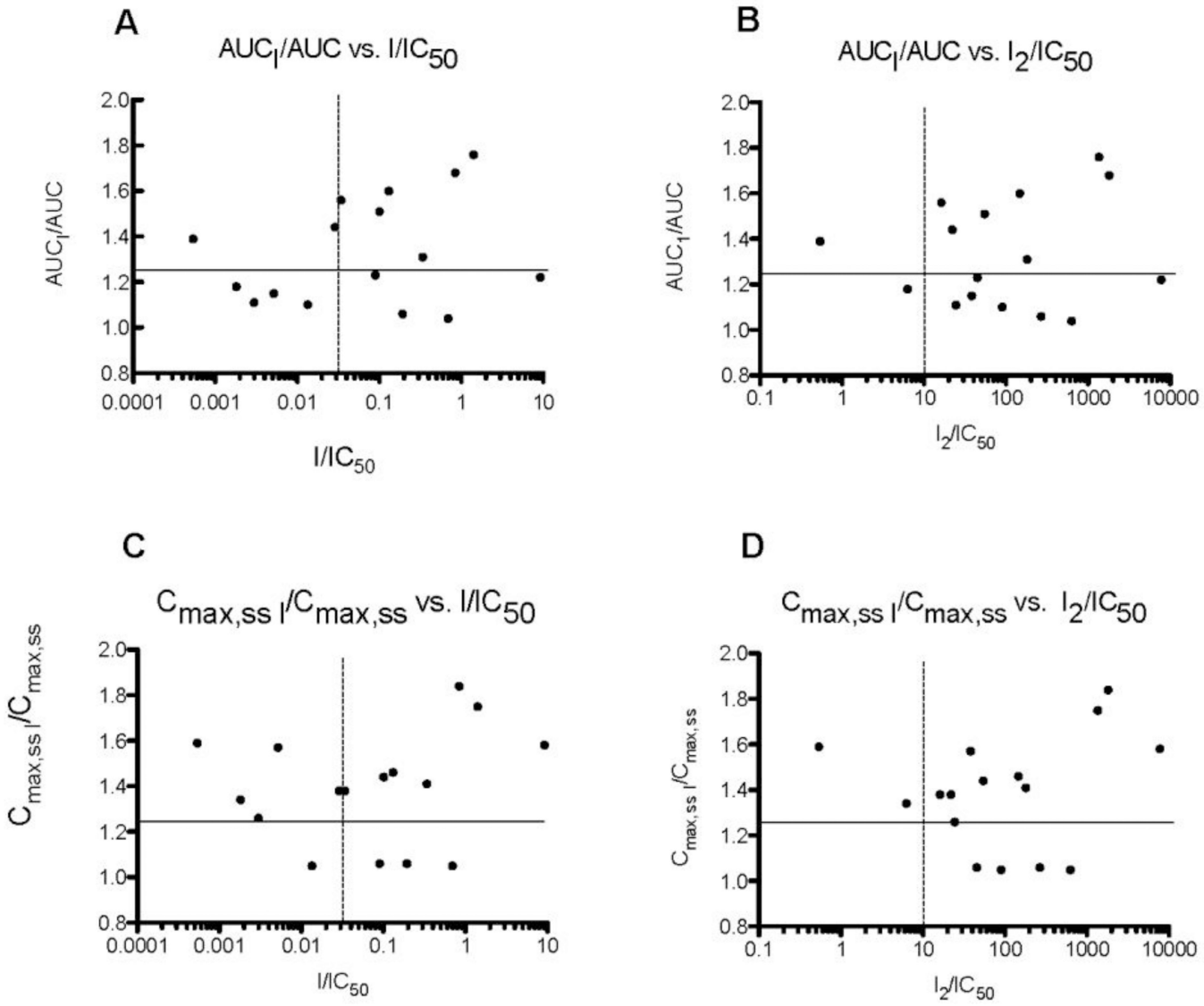

Fig. 7.

(a) Plot of the ratio of AUC for digoxin in the presence and absence of drug (inhibitor) vs. the ratio of peak plasma concentration of drug (inhibitor) and the IC_{50} for Fl-*t*-pgp. (b) Plot of the ratio of AUC for digoxin in the presence and absence of drug (inhibitor) vs. the ratio of gastrointestinal concentration of drug (inhibitor) and the IC_{50} for Fl-*t*-pgp. (c) Plot of the ratio of C_{max} for digoxin in the presence and absence of drug (inhibitor) vs. the ratio of peak plasma concentration of drug (inhibitor) and the IC_{50} for Fl-*t*-pgp. (d) Plot of the ratio of C_{max} for digoxin in the presence and absence of drug (inhibitor) vs. the ratio of gastrointestinal concentration of drug (inhibitor) and the IC_{50} for Fl-*t*-pgp. *In vivo* data are taken from Fenner et al. (Fenner et al., 2009).

Table 1

Pgp IC_{50} values for test compounds determined by Fl-*t*-pgp and by LLC-MDR1 cell monolayers, and the K_d for binding of various test compounds (all in μM).

Test compound	IC_{50} Fl-*t*-pgp[a]	K_d[b]	IC_{50} LLC-MDR1[c]
Tariquidar	0.021		
Elacridar	0.10	0.59	
Telmisartan	0.12		17
Ritonavir	0.25	0.79	18
Valspodar	0.25	0.08	
Reserpine	0.31	0.73	
Cyclosporin A	0.58	0.3	1.4
Nelfinavir	0.59	0.98	
Zosuquidar	0.59	0.055	
Indinavir	0.93	0.94	
Nicardipine	0.93	6.5	11
Paclitaxel	1.2	0.038	
Ketoconazole	2.0	2.5	3.4
Ivermectin	2.5	2.5	
Quinidine HCl	2.5	7.8	56
Nifedipine	2.6	48	
Amiodarone	2.6	2	21
Progesterone	3.7	0.9	
Carvedilol	3.8		32
Troglitazone	5.2		12
Nitrendipine	5.8	7.1	
Simvastatin lactone	6.0		
Isradipine	6.6	13	29
Mibefradil	7.1		11
Ko143	7.5		
Verapamil HCl	9.1	2.4	57
Vinblastine	9.5	2.9	
NAc-LLY-amide	13	28	
Tamoxifen	14	4.1	
Trifluoperazine	15	7.7	
Felopidine	17	4.3	17
Simvastatin acid	20		
Sulfinpyrazone	23	24	
Diltiazem	24		83
Pepstatin A	29	36	
Sertraline	29	37	
Benzbromarone	44		
Indomethacin	51	36	

Test compound	IC_{50} Fl-*t*-pgp[a]	K_d[b]	IC_{50} LLC-MDR1[c]
Ranolazine	64		130
Digoxin	80	53	
ALLN	140	83	
Naloxone	210	54	
Colchicine	230	160	
Probenecid	240		
Captopril	430		>1000
Digoxigenin	520	260	

[a] Determined using the Fl-*t*-pgp inhibition assay

[b] Determined using fluorescence quenching of purified Pgp

[c] Determined using inhibition of net transport of [^{3}H]digoxin in LLC-MDR1 cell monolayers

Table 2

Data for correlations of IC_{50} values for various drugs determined using Fl-*t*-pgp with *in vivo* effects on digoxin disposition in humans

	Digoxin *in vivo*		[inhibitor] *in vivo*		Fl-*t*-pgp		
Drug	**AUC_I/AUC**	**$C_{max,ss,I}/C_{max,ss}$**	**[I]**[a]	**$[I_2]$**[b]	**$IC_{50,Fl}$**[c]	**$[I]/IC_{50,Fl}$**	**$[I_2]/IC_{50,Fl}$**
Diltiazem	1.44	1.38	0.7	532	24.2	0.02893	21.98
Quinidine	1.76	1.75	3.54	3397	2.5	1.416	1359
Telmisartan	1.22	1.58	1.11	933	0.12	9.250	7775
Troglitazone	1.04	1.05	3.62	3264	5.2	0.6961	627.7
Verapamil	1.51	1.44	1.2	652	11.9	0.1008	54.79
Carvedilol	1.56	1.38	0.13	61.5	3.8	0.03421	16.18
Felodipine	1.18	1.34	0.03	104	16.5	0.001818	6.303
Mibefradil	1.31	1.41	2.42	1211	7.1	0.3408	179.0
Nicardipine	1.06	1.06	0.18	248	0.93	0.194	266.7
Ranolazine	1.6	1.46	8.4	9356	64.1	0.1310	146.0
Amiodarone	1.68	1.84	2.2	4693	2.6	0.8461	1805
Isradipine	1.11	1.26	0.02	161.5	6.6	0.003030	24.47
Sertraline	1.1	1.05	0.39	2612	29	0.01345	90.07
Captopril	1.39	1.59	0.23	230	429	0.0005361	0.5361
Nifedipine	1.23	1.06	0.23	115.5	2.6	0.08846	44.42
Nitrendipine	1.15	1.57	0.03	222.0	5.8	0.005172	38.28

[a] Peak plasma concentration of drug ("inhibitor") at steady state, in µM; data taken from Fenner et al. (Fenner et al., 2009).

[b] Estimated gastrointestinal concentration of drug ("inhibitor") after oral dose, in µM; data taken from Fenner et al. (Fenner et al., 2009).

[c] Half-maximal concentration for inhibition of transport in Fl-*t*-pgp by drug ("inhibitor"), in µM.